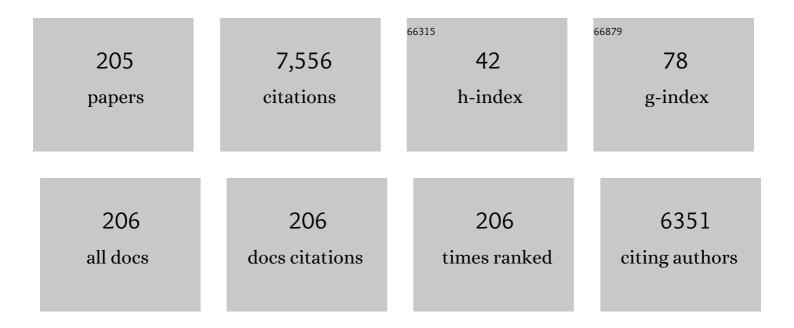
List of Publications by Year in descending order

Source: https://exaly.com/author-pdf/8091880/publications.pdf Version: 2024-02-01



#	Article	IF	CITATIONS
1	New Developments of Ti-Based Alloys for Biomedical Applications. Materials, 2014, 7, 1709-1800.	1.3	756
2	Microstructure and compressive properties of AlCrFeCoNi high entropy alloy. Materials Science & Engineering A: Structural Materials: Properties, Microstructure and Processing, 2008, 491, 154-158.	2.6	413
3	Distinction in corrosion resistance of selective laser melted Ti-6Al-4V alloy on different planes. Corrosion Science, 2016, 111, 703-710.	3.0	325
4	Oxygen Vacancy Promoted Heterogeneous Fenton-like Degradation of Ofloxacin at pH 3.2–9.0 by Cu Substituted Magnetic Fe ₃ O ₄ @FeOOH Nanocomposite. Environmental Science & Technology, 2017, 51, 12699-12706.	4.6	273
5	Effects of Mn, Ti and V on the microstructure and properties of AlCrFeCoNiCu high entropy alloy. Materials Science & Engineering A: Structural Materials: Properties, Microstructure and Processing, 2008, 498, 482-486.	2.6	213
6	Effect of Powder Particle Shape on the Properties of In Situ Ti–TiB Composite Materials Produced by Selective Laser Melting. Journal of Materials Science and Technology, 2015, 31, 1001-1005.	5.6	201
7	Surface aging behaviour of Fe-based amorphous alloys as catalysts during heterogeneous photo Fenton-like process for water treatment. Applied Catalysis B: Environmental, 2017, 204, 537-547.	10.8	173
8	Disordered Atomic Packing Structure of Metallic Glass: Toward Ultrafast Hydroxyl Radicals Production Rate and Strong Electron Transfer Ability in Catalytic Performance. Advanced Functional Materials, 2017, 27, 1702258.	7.8	160
9	A Review on Highâ€Strength Titanium Alloys: Microstructure, Strengthening, and Properties. Advanced Engineering Materials, 2019, 21, 1801359.	1.6	144
10	Ultrahigh-performance TiNi shape memory alloy by 4D printing. Materials Science & Engineering A: Structural Materials: Properties, Microstructure and Processing, 2019, 763, 138166.	2.6	122
11	Biomimetic Diselenideâ€Bridged Mesoporous Organosilica Nanoparticles as an Xâ€rayâ€Responsive Biodegradable Carrier for Chemoâ€Immunotherapy. Advanced Materials, 2020, 32, e2004385.	11.1	122
12	Bimodal titanium alloys with ultrafine lamellar eutectic structure fabricated by semi-solid sintering. Acta Materialia, 2017, 132, 491-502.	3.8	117
13	Comparative study of microstructures and mechanical properties of in situ Ti–TiB composites produced by selective laser melting, powder metallurgy, and casting technologies. Journal of Materials Research, 2014, 29, 1941-1950.	1.2	116
14	Enhanced peroxymonosulfate activation for phenol degradation over MnO2 at pH 3.5–9.0 via Cu(II) substitution. Journal of Hazardous Materials, 2018, 360, 303-310.	6.5	111
15	Chemical speciation of fine particle bound trace metals. International Journal of Environmental Science and Technology, 2009, 6, 337-346.	1.8	110
16	Stable tensile recovery strain induced by a Ni4Ti3 nanoprecipitate in a Ni50.4Ti49.6 shape memory alloy fabricated via selective laser melting. Acta Materialia, 2021, 219, 117261.	3.8	98
17	Ultrafine grained Ti-based composites with ultrahigh strength and ductility achieved by equiaxing microstructure. Materials & Design, 2015, 79, 1-5.	5.1	89
18	Simultaneous enhancement of mechanical and shape memory properties by heat-treatment homogenization of Ti2Ni precipitates in TiNi shape memory alloy fabricated by selective laser melting. Journal of Materials Science and Technology, 2022, 101, 205-216.	5.6	89

#	Article	IF	CITATIONS
19	Carbon doped molybdenum disulfide nanosheets stabilized on graphene for the hydrogen evolution reaction with high electrocatalytic ability. Nanoscale, 2016, 8, 1676-1683.	2.8	88
20	Overcoming the strength–ductility trade-off by tailoring grain-boundary metastable Si-containing phase in β-type titanium alloy. Journal of Materials Science and Technology, 2021, 68, 112-123.	5.6	87
21	A nanoparticulate dual scavenger for targeted therapy of inflammatory bowel disease. Science Advances, 2022, 8, eabj2372.	4.7	87
22	Premature failure of an additively manufactured material. NPG Asia Materials, 2020, 12, .	3.8	81
23	A DAMP-scavenging, IL-10-releasing hydrogel promotes neural regeneration and motor function recovery after spinal cord injury. Biomaterials, 2022, 280, 121279.	5.7	73
24	Influence of powder properties on densification mechanism during spark plasma sintering. Scripta Materialia, 2017, 139, 96-99.	2.6	72
25	Bulk WC–Al2O3 composites prepared by spark plasma sintering. International Journal of Refractory Metals and Hard Materials, 2012, 30, 51-56.	1.7	71
26	In-situ alloyed, oxide-dispersion-strengthened CoCrFeMnNi high entropy alloy fabricated via laser powder bed fusion. Materials and Design, 2020, 194, 108966.	3.3	69
27	Copper in LaMnO3 to promote peroxymonosulfate activation by regulating the reactive oxygen species in sulfamethoxazole degradation. Journal of Hazardous Materials, 2021, 411, 125163.	6.5	65
28	Densification mechanism of Ti-based metallic glass powders during spark plasma sintering process. Intermetallics, 2015, 66, 1-7.	1.8	64
29	Biomedical TiNbZrTaSi alloys designed by d-electron alloy design theory. Materials and Design, 2015, 85, 7-13.	3.3	64
30	High-strength silicon brass manufactured by selective laser melting. Materials Letters, 2018, 210, 169-172.	1.3	63
31	Fabrication, performance and mechanism of MgO meso-/macroporous nanostructures for simultaneous removal of As(<scp>iii</scp>) and F in a groundwater system. Environmental Science: Nano, 2016, 3, 1416-1424.	2.2	61
32	Bimorphic microstructure in Ti-6Al-4V alloy manipulated by spark plasma sintering and in-situ press forging. Scripta Materialia, 2021, 193, 43-48.	2.6	58
33	Heterogeneous photo Fenton-like degradation of cibacron brilliant red 3B-A dye using amorphous Fe 78 Si 9 B 13 and Fe 73.5 Si 13.5 B 9 Cu 1 Nb 3 alloys: The influence of adsorption. Journal of the Taiwan Institute of Chemical Engineers, 2017, 71, 128-136.	2.7	57
34	ZrO2 (3Y) toughened WC composites prepared by spark plasma sintering. Journal of Alloys and Compounds, 2013, 572, 62-67.	2.8	56
35	A novel high-strength Al-based nanocomposite reinforced with Ti-based metallic glass nanoparticles produced by powder metallurgy. Materials Science & Engineering A: Structural Materials: Properties, Microstructure and Processing, 2018, 734, 34-41.	2.6	56
36	(SiCp+Ti)/7075Al hybrid composites with high strength and large plasticity fabricated by squeeze casting. Materials Science & Engineering A: Structural Materials: Properties, Microstructure and Processing, 2014, 609, 250-254.	2.6	55

#	Article	IF	CITATIONS
37	Ultrafine-grained Ti-based composites with high strength and low modulus fabricated by spark plasma sintering. Materials Science & amp; Engineering A: Structural Materials: Properties, Microstructure and Processing, 2013, 560, 857-861.	2.6	52
38	Well-dispersed magnetic iron oxide nanocrystals on sepiolite nanofibers for arsenic removal. RSC Advances, 2015, 5, 25236-25243.	1.7	50
39	Improving the Mechanical Properties of Cu-15Ni-8Sn Alloys by Addition of Titanium. Materials, 2017, 10, 1038.	1.3	49
40	Biomimetic co-assembled nanodrug of doxorubicin and berberine suppresses chemotherapy-exacerbated breast cancer metastasis. Biomaterials, 2021, 271, 120716.	5.7	49
41	Equiaxed Ti-based composites with high strength and large plasticity prepared by sintering and crystallizing amorphous powder. Materials Science & Engineering A: Structural Materials: Properties, Microstructure and Processing, 2016, 650, 171-182.	2.6	48
42	Nucleation and growth mechanism of crystalline phase for fabrication of ultrafine-grained Ti66Nb13Cu8Ni6.8Al6.2 composites by spark plasma sintering and crystallization of amorphous phase. Materials Science & Engineering A: Structural Materials: Properties, Microstructure and Processing, 2010, 528, 486-493.	2.6	47
43	Fabrication of biomedical Ti–35Nb–7Zr–5Ta alloys by mechanical alloying and spark plasma sintering. Powder Metallurgy, 2012, 55, 65-70.	0.9	44
44	Non-isothermal and isothermal crystallization kinetics and their effect on microstructure of sintered and crystallized TiNbZrTaSi bulk alloys. Journal of Non-Crystalline Solids, 2016, 432, 440-452.	1.5	43
45	Reaction diffusion rate coefficient derivation by isothermal heat treatment in spark plasma sintering system. Scripta Materialia, 2017, 134, 91-94.	2.6	42
46	Preliminary investigation of chloramphenicol in fish, water and sediment from freshwater aquaculture pond. International Journal of Environmental Science and Technology, 2009, 6, 597-604.	1.8	41
47	Densification and microstructure evolution during SPS consolidation process in W-Ni-Fe system. Transactions of Nonferrous Metals Society of China, 2011, 21, 493-501.	1.7	41
48	Determination of atomic diffusion coefficient via isochronal spark plasma sintering. Scripta Materialia, 2018, 151, 47-52.	2.6	41
49	Facile synthesis of hierarchical dendrite-like structure iron layered double hydroxide nanohybrids for effective arsenic removal. Chemical Communications, 2016, 52, 11955-11958.	2.2	40
50	Coordination and Redox Dualâ€Responsive Mesoporous Organosilica Nanoparticles Amplify Immunogenic Cell Death for Cancer Chemoimmunotherapy. Small, 2021, 17, e2100006.	5.2	40
51	93W–5.6Ni–1.4Fe heavy alloys with enhanced performance prepared by cyclic spark plasma sintering. Materials Science & Engineering A: Structural Materials: Properties, Microstructure and Processing, 2014, 599, 233-241.	2.6	39
52	Microstructure, shape memory properties, and inÂvitro biocompatibility of porous NiTi scaffolds fabricated via selective laser melting. Journal of Materials Research and Technology, 2021, 15, 6797-6812.	2.6	36
53	Ultrafine-grained Ti ₆₆ Nb ₁₃ Cu ₈ Ni _{6.8} Al _{6.2} composites fabricated by spark plasma sintering and crystallization of amorphous phase. Journal of Materials Research, 2009, 24, 2118-2122.	1.2	35
54	Intrinsic relationship between crystallization mechanism of metallic glass powder and microstructure of bulk alloys fabricated by powder consolidation and crystallization of amorphous phase. Journal of Alloys and Compounds, 2014, 586, 542-548.	2.8	34

#	Article	lF	CITATIONS
55	Novel Colorimetric Method for Simultaneous Detection and Identification of Multimetal Ions in Water: Sensitivity, Selectivity, and Recognition Mechanism. ACS Omega, 2019, 4, 5915-5922.	1.6	34
56	Effect of ultrasonic surface rolling on surface layer properties and fretting wear properties of titanium alloy Ti5Al4Mo6V2Nb1Fe. Surface and Coatings Technology, 2020, 389, 125612.	2.2	34
57	Effects of brazing temperature and testing temperature on the microstructure and shear strength of γ-TiAl joints. Materials Science & Engineering A: Structural Materials: Properties, Microstructure and Processing, 2015, 634, 91-98.	2.6	33
58	Effect of Fe content on glass-forming ability and crystallization behavior of a (Ti69.7Nb23.7Zr4.9Ta1.7)100â^'xFex alloy synthesized by mechanical alloying. Journal of Alloys and Compounds, 2013, 553, 40-47.	2.8	32
59	Equiaxed grained structure: A structure in titanium alloys with higher compressive mechanical properties. Materials Science & Engineering A: Structural Materials: Properties, Microstructure and Processing, 2013, 580, 397-405.	2.6	32
60	A versatile logic detector and fluorescent film based on Eu-based MOF for swift detection of formaldehyde in solutions and gas phase. Journal of Hazardous Materials, 2021, 410, 124624.	6.5	32
61	An Injectable Antibiotic Hydrogel that Scavenges Proinflammatory Factors for the Treatment of Severe Abdominal Trauma. Advanced Functional Materials, 2022, 32, .	7.8	32
62	Tannic Acid-Assisted Synthesis of Biodegradable and Antibacterial Mesoporous Organosilica Nanoparticles Decorated with Nanosilver. ACS Sustainable Chemistry and Engineering, 2020, 8, 1695-1702.	3.2	31
63	Achieving ultrahigh-strength in beta-type titanium alloy by controlling the melt pool mode in selective laser melting. Materials Science & Engineering A: Structural Materials: Properties, Microstructure and Processing, 2021, 823, 141731.	2.6	31
64	Effects of metallic Ti particles on the aging behavior and the influenced mechanical properties of squeeze-cast (SiCp+Ti)/7075Al hybrid composites. Materials Science & Engineering A: Structural Materials: Properties, Microstructure and Processing, 2015, 620, 190-197.	2.6	30
65	Cancer–leukocyte hybrid membrane-cloaked magnetic beads for the ultrasensitive isolation, purification, and non-destructive release of circulating tumor cells. Nanoscale, 2020, 12, 19121-19128.	2.8	30
66	Efficient fenton-like degradation of ofloxacin over bimetallic Fe–Cu@Sepiolite composite. Chemosphere, 2020, 257, 127209.	4.2	30
67	Bioactive Injectable Hydrogel Dressings for Bacteria-Infected Diabetic Wound Healing: A "Pull–Push― Approach. ACS Applied Materials & Interfaces, 2022, 14, 26404-26417.	4.0	30
68	Effect of Si and Ti on dynamic recrystallization of high-performance Cuâ^15Niâ^18Sn alloy during hot deformation. Transactions of Nonferrous Metals Society of China, 2019, 29, 2556-2565.	1.7	29
69	Zirconia-toughened WC with/without VC and Cr3C2. Ceramics International, 2014, 40, 2011-2016.	2.3	28
70	A new insight into high-strength Ti62Nb12.2Fe13.6Co6.4Al5.8 alloys with bimodal microstructure fabricated by semi-solid sintering. Scientific Reports, 2016, 6, 23467.	1.6	28
71	Safe and efficient degradation of metronidazole using highly dispersed β-FeOOH on palygorskite as heterogeneous Fenton-like activator of hydrogen peroxide. Chemosphere, 2019, 236, 124367.	4.2	28
72	Effect of heat treatments on the microstructure and mechanical properties of Ti2AlNb intermetallic fabricated by selective laser melting. Materials Science & Engineering A: Structural Materials: Properties, Microstructure and Processing, 2021, 817, 141352.	2.6	28

#	Article	IF	CITATIONS
73	Effect of WC content on glass formation, thermal stability, and phase evolution of a TiNbCuNiAl alloy synthesized by mechanical alloying. Journal of Materials Research, 2008, 23, 745-754.	1.2	27
74	Influence of powder shape on atomic diffusivity and resultant densification mechanisms during spark plasma sintering. Journal of Alloys and Compounds, 2019, 802, 600-608.	2.8	27
75	Additive manufacturing of a martensitic Co–Cr–Mo alloy: Towards circumventing the strength–ductility trade-off. Additive Manufacturing, 2021, 37, 101725.	1.7	27
76	Adsorption behavior of methylene blue on amine-functionalized ordered mesoporous alumina. Journal of Porous Materials, 2015, 22, 147-155.	1.3	26
77	High‣trength AlCrFeCoNi High Entropy Alloys Fabricated by Using Metallic Glass Powder as Precursor. Advanced Engineering Materials, 2016, 18, 348-353.	1.6	26
78	In-situ elongated β-Si3N4 grains toughened WC composites prepared by one/two-step spark plasma sintering. Materials Science & Engineering A: Structural Materials: Properties, Microstructure and Processing, 2013, 561, 445-451.	2.6	25
79	Effect of Si on Fe-rich intermetallic formation and mechanical properties of heat-treated Al–Cu–Mn–Fe alloys. Journal of Materials Research, 2018, 33, 898-911.	1.2	25
80	Effect of Si addition and applied pressure on microstructure and tensile properties of as-cast Al-5.0Cu-0.6Mn-1.2Fe alloys. Transactions of Nonferrous Metals Society of China, 2018, 28, 1061-1072.	1.7	25
81	Potential superhard cubic spinel CSi2N4: First-principles investigations. Journal of Applied Physics, 2008, 103, .	1.1	24
82	Effect of minor Cu content on microstructure and mechanical property of NiTiCu bulk alloys fabricated by crystallization of metallic glass powder. Intermetallics, 2015, 56, 37-43.	1.8	24
83	Microstructure and mechanical property of bimodal-size metallic glass particle-reinforced Al alloy matrix composites. Journal of Alloys and Compounds, 2020, 814, 152317.	2.8	24
84	Correlation between atomic diffusivity and densification mechanism during spark plasma sintering of titanium alloy powders. Journal of Alloys and Compounds, 2019, 787, 112-122.	2.8	23
85	Superior Wear Resistance in EBM-Processed TC4 Alloy Compared with SLM and Forged Samples. Materials, 2019, 12, 782.	1.3	23
86	Near-infrared light-responsive hybrid hydrogels for the synergistic chemo-photothermal therapy of oral cancer. Nanoscale, 2021, 13, 17168-17182.	2.8	23
87	Oxygen-induced amorphization of metallic titanium by ball milling. Journal of Materials Research, 2007, 22, 1927-1932.	1.2	22
88	Designing ultrafine lamellar eutectic structure in bimodal titanium alloys by semi-solid sintering. Journal of Alloys and Compounds, 2017, 702, 51-59.	2.8	21
89	Effect of Zr addition on the microstructure and tribological property of the anodization of Ti-6Al-4V alloy. Surface and Coatings Technology, 2018, 356, 38-48.	2.2	21
90	Large tensile plasticity in Zr-based metallic glass/stainless steel interpenetrating-phase composites prepared by high pressure die casting. Composites Part B: Engineering, 2021, 224, 109226.	5.9	21

#	Article	IF	CITATIONS
91	Effects of particle size and properties on the microstructures, mechanical properties, and fracture mechanisms of 7075Al hybrid composites prepared by squeeze casting. Journal of Materials Science, 2014, 49, 7855-7863.	1.7	20
92	Ductile fine-grained Ti–O-based composites with ultrahigh compressive specific strength fabricated by spark plasma sintering. Materials Science & Engineering A: Structural Materials: Properties, Microstructure and Processing, 2011, 528, 1897-1900.	2.6	19
93	Friction welding of electron beam melted Ti-6Al-4V. Materials Science & Engineering A: Structural Materials: Properties, Microstructure and Processing, 2019, 761, 138045.	2.6	19
94	More reactive oxygen species generation facilitated by highly dispersed bimodal gold nanoparticle on the surface of Bi2WO6 for enhanced photocatalytic degradation of ofloxacin in water. Chemosphere, 2021, 269, 128717.	4.2	19
95	Ti-based bulk metallic glass matrix composites with in situ precipitated β-Ti phase fabricated by spark plasma sintering. Journal of Non-Crystalline Solids, 2013, 359, 15-20.	1.5	18
96	Crystallization kinetics and spark plasma sintering of amorphous Ni53Nb20Ti10Zr8Co6Ta3 powders prepared by mechanical alloying. Vacuum, 2015, 114, 93-100.	1.6	18
97	Microstructure and electrochemical corrosion behavior of selective laser melted Tiâ^'6Alâ^'4V alloy in simulated artificial saliva. Transactions of Nonferrous Metals Society of China, 2021, 31, 167-177.	1.7	18
98	Altered phase transformation behaviors and enhanced bending shape memory property of NiTi shape memory alloy via selective laser melting. Journal of Materials Processing Technology, 2022, 303, 117546.	3.1	18
99	Cr3C2 and VC doped WC–Si3N4 composites prepared by spark plasma sintering. International Journal of Refractory Metals and Hard Materials, 2013, 41, 540-546.	1.7	17
100	Machining performance of a grooved tool in dry machining Ti-6Al-4ÂV. International Journal of Advanced Manufacturing Technology, 2014, 73, 613-622.	1.5	17
101	Texture evolution and mechanical behavior of commercially pure Ti processed via pulsed electric current treatment. Journal of Materials Science, 2016, 51, 10608-10619.	1.7	17
102	High-strength and free-cutting silicon brasses designed via the zinc equivalent rule. Materials Science & Engineering A: Structural Materials: Properties, Microstructure and Processing, 2018, 723, 296-305.	2.6	17
103	Revealing dehydrogenation effect and resultant densification mechanism during pressureless sintering of TiH2 powder. Journal of Alloys and Compounds, 2021, 873, 159792.	2.8	17
104	Constructing function domains in NiTi shape memory alloys by additive manufacturing. Virtual and Physical Prototyping, 2022, 17, 563-581.	5.3	17
105	Formation of Fe–Nb–X (X=Zr, Ti) amorphous alloys from pure metal elements by mechanical alloying. Physica B: Condensed Matter, 2012, 407, 258-262.	1.3	16
106	Bimodal eutectic titanium alloys: Microstructure evolution, mechanical behavior and strengthening mechanism. Materials Science & Engineering A: Structural Materials: Properties, Microstructure and Processing, 2017, 700, 10-18.	2.6	16
107	Significant enhancement of photo-Fenton degradation of ofloxacin over Fe-Dis@Sep due to highly dispersed FeC6 with electron deficiency. Science of the Total Environment, 2020, 723, 138144.	3.9	16
108	Effect of V content on microstructure and mechanical property of a TiVCuNiAl composite fabricated by spark plasma sintering. Materials & Design, 2013, 52, 655-662.	5.1	15

#	Article	IF	CITATIONS
109	Biomedical porous TiNbZrFe alloys fabricated using NH ₄ HCO ₃ as pore forming agent through powder metallurgy route. Powder Metallurgy, 2015, 58, 228-234.	0.9	15
110	Ultrafast consolidation of bulk nanocrystalline titanium alloy through ultrasonic vibration. Scientific Reports, 2018, 8, 801.	1.6	15
111	Machining performance of PCD and PCBN tools in dry turning titanium alloy Ti-6Al-0.6Cr-0.4Fe-0.4Si-0.01B. International Journal of Advanced Manufacturing Technology, 2019, 102, 2649-2661.	1.5	15
112	Carbon dots–MnO ₂ nanocomposites for As(<scp>iii</scp>) detection in groundwater with high sensitivity and selectivity. Analytical Methods, 2020, 12, 5572-5580.	1.3	15
113	The effect of electric pulse aided ultrasonic rolling processing on the microstructure evolution, surface properties, and fatigue properties of a titanium alloy Ti5Al4Mo6V2Nb1Fe. Surface and Coatings Technology, 2021, 421, 127408.	2.2	15
114	Bulk TiB2-Based Ceramic Composites with Improved Mechanical Property Using Fe–Ni–Ti–Al as a Sintering Aid. Materials, 2014, 7, 7105-7117.	1.3	14
115	Microstructure evolution and superelasticity of Ti-24Nb-xZr alloys fabricated by spark plasma sintering. Journal of Alloys and Compounds, 2020, 823, 153875.	2.8	14
116	Nanosilver-Decorated Biodegradable Mesoporous Organosilica Nanoparticles for GSH-Responsive Gentamicin Release and Synergistic Treatment of Antibiotic-Resistant Bacteria. International Journal of Nanomedicine, 2021, Volume 16, 4631-4642.	3.3	14
117	Formation of ZrTiCuNiBe bulk metallic glass by shock-wave quenching. Applied Physics Letters, 2005, 87, 051904.	1.5	13
118	Microstructure and magnetic properties of anisotropic Nd–Fe–B magnets prepared by spark plasma sintering and hot deformation. Transactions of Nonferrous Metals Society of China, 2014, 24, 3142-3151.	1.7	13
119	Improved mechanical properties of biomedical ZrNbHf alloy induced by oxidation treatment. Materials & Design, 2015, 78, 25-32.	5.1	13
120	Machining Performance of TiAlN-Coated Cemented Carbide Tools with Chip Groove in Machining Titanium Alloy Ti-6Al-0.6Cr-0.4Fe-0.4Si-0.01B. Metals, 2018, 8, 850.	1.0	13
121	Surface deep oxidation of ofloxacin and 2,4-dichlorophenol over ferrocene@sepiolite due to their synergistic effect in visible light driven heterogeneous Fenton reaction process. Environmental Science: Nano, 2018, 5, 1943-1950.	2.2	13
122	Achieving super-high strength in an aluminum based composite by reinforcing metallic glassy flakes. Materials Letters, 2020, 262, 127059.	1.3	13
123	Sulfur quantum dot-based portable paper sensors for fluorometric and colorimetric dual-channel detection of cobalt. Journal of Materials Science, 2021, 56, 4782-4796.	1.7	13
124	Effect of silicon content on the microstructure evolution, mechanical properties, and biocompatibility of β-type TiNbZrTa alloys fabricated by laser powder bed fusion. Materials Science and Engineering C, 2022, 133, 112625.	3.8	13
125	Improvement in tensile plasticity of pressureless-sintered TiBw/Ti composites by evading Kirkendall's pore. Powder Technology, 2022, 396, 444-448.	2.1	12
126	Rapid and sensitive screening of multiple polycyclic aromatic hydrocarbons by a reusable fluorescent sensor array. Journal of Hazardous Materials, 2022, 424, 127694.	6.5	12

#	Article	IF	CITATIONS
127	Void formation and cracking of Zr41Ti14Cu12.5- Ni10Be22.5 bulk metallic glass under planar shock compression. Journal of Materials Science, 2005, 40, 3917-3920.	1.7	11
128	High speed impact on Zr41Ti14Cu12.5Ni10Be22.5 bulk metallic glass. Materials Science & Engineering A: Structural Materials: Properties, Microstructure and Processing, 2006, 426, 298-304.	2.6	11
129	Unusual dry sliding tribological behavior of biomedical ultrafine-grained TiNbZrTaFe composites fabricated by powder metallurgy. Journal of Materials Research, 2014, 29, 902-909.	1.2	11
130	A carbon-dot-based dual-emission probe for ultrasensitive visual detection of copper ions. New Journal of Chemistry, 2018, 42, 19771-19778.	1.4	11
131	Fabrication of highly dissimilar TC4/steel joint with V/Cu composite transition layer by laser melting deposition. Journal of Alloys and Compounds, 2021, 862, 158319.	2.8	11
132	Damage Features of Zr41Ti14Cu12.5Ni10Be22.5 Bulk Metallic Glass Impacted by Hypervelocity Projectiles. Journal of Spacecraft and Rockets, 2006, 43, 565-567.	1.3	10
133	An Innovative Approach to Separate Iron Oxide Concentrate from High-sulfur and Low-grade Pyrite Cinders. Journal of Iron and Steel Research International, 2016, 23, 756-764.	1.4	10
134	Influence of In content on physical properties of β-type TiNbZrIn powders prepared by mechanical alloying. Vacuum, 2018, 151, 175-181.	1.6	10
135	Crystallization of Zr41Ti14Cu12.5Ni10Be22.5 bulk metallic glass under high pressure examined byin situsynchrotron radiation x-ray diffraction. Journal of Applied Physics, 2006, 99, 023525.	1.1	9
136	Microstructure and Mechanical Properties of SPSed (Spark Plasma Sintered) Ti ₆₆ Nb ₁₃ Cu ₈ Ni _{6.8} Al _{6.2} Bulk Alloys with and without WC Addition. Materials Transactions, 2009, 50, 1720-1724.	0.4	9
137	Microstructure evolution and thermal properties in FeMoPCB alloy during mechanical alloying. Journal of Non-Crystalline Solids, 2012, 358, 1459-1464.	1.5	9
138	Bulk multimodal-grained irons with large plasticity fabricated by spark plasma sintering. Materials Science & Engineering A: Structural Materials: Properties, Microstructure and Processing, 2014, 591, 54-58.	2.6	9
139	Effects of sintering parameters on the microstructure and mechanical properties of carbon nanotubes reinforced aluminum matrix composites. Journal of Materials Research, 2016, 31, 3757-3765.	1.2	9
140	Comparison of TiAlâ€Based Intermetallics Joints Brazed with Amorphous and Crystalline Ti–Zr–Cu–Ni–Co–Mo Fillers. Advanced Engineering Materials, 2016, 18, 341-347.	1.6	9
141	Construction of salicylaldehyde analogues as turn-on fluorescence probes and their electronic effect on sensitive and selective detection of As(<scp>v</scp>) in groundwater. Analytical Methods, 2019, 11, 955-964.	1.3	9
142	One-pot synthesis of chlorhexidine-templated biodegradable mesoporous organosilica nanoantiseptics. Colloids and Surfaces B: Biointerfaces, 2020, 187, 110653.	2.5	9
143	Abnormal hot deformation behavior in a metallic-glass-reinforced Al-7075 composite. Materials Science & Engineering A: Structural Materials: Properties, Microstructure and Processing, 2020, 785, 139212.	2.6	9
144	Insight into enhanced Fenton-like degradation of antibiotics over CuFeO2 based nanocomposite: To improve the utilization efficiency of OH/O2- via minimizing its migration distance. Chemosphere, 2022, 294, 133743.	4.2	9

#	Article	IF	CITATIONS
145	Scalable biomimetic SARS-CoV‑2 nanovaccines with robust protective immune responses. Signal Transduction and Targeted Therapy, 2022, 7, 96.	7.1	9
146	Research on Binderless Tungsten Carbide Prepared by Spark Plasma Sintering. Applied Mechanics and Materials, 2010, 37-38, 980-984.	0.2	8
147	Tough TiB ₂ â€Based Ceramic Composites Using Metallic Glass Powder as the Sintering Aid. Advanced Engineering Materials, 2016, 18, 1936-1943.	1.6	8
148	Effective atomic diffusion coefficient dependence on applied pressure during spark plasma sintering. Materialia, 2019, 6, 100334.	1.3	8
149	Microstructure and mechanical properties of TiAl/Ni-based superalloy joints vacuum brazed with Ti–Zr–Fe–Cu–Ni–Co–Mo filler metal. Rare Metals, 2021, 40, 2134-2142.	3.6	8
150	Portable smartphone-integrated paper sensors for fluorescence detection of As(III) in groundwater. Royal Society Open Science, 2020, 7, 201500.	1.1	8
151	Bonding mechanism of X10CrNi18-8 with Ni/Al2O3 composite ceramic by pressureless infiltration. Central South University, 2011, 18, 953-959.	0.5	7
152	Effects of Unreacted Ti Particles on the Dry Sliding Tribological Behavior of Squeeze-Cast (SiCpÂ+ÂTi)/7075Al Hybrid Composites Under Different Applied Loads. Tribology Letters, 2017, 65, 1.	1.2	7
153	Interface Structure and Mechanical Properties of 7075Al Hybrid Composite Reinforced with Micron Ti Metal Particles Using Pressure Infiltration. Metals, 2019, 9, 763.	1.0	7
154	Comparative analysis of the hot-isostatic-pressing densification behavior of atomized and milled Ti6Al4V powders. Journal of Materials Research and Technology, 2020, 9, 3091-3108.	2.6	7
155	High Plastic Ti ₆₆ Nb ₁₃ Cu ₈ Ni _{6.8} Al _{6.2} Composites with <i>In Situ</i> β-Ti Phase Synthesized by Spark Plasma Sintering of Mechanically Alloyed Glassy Powders. Materials Science Forum, 2010, 638-642, 1642-1647.	0.3	6
156	Fabrication of Ultrafine-Grained Ti ₆₆ Nb ₁₈ Cu _{6.4} Ni _{6.1Composites with High Strength and Distinct Plasticity by Spark Plasma Sintering and Crystallization of Amorphous Phase. Materials Transactions, 2012, 53, 531-536.}	gt:Al <s< td=""><td>ub>3.5<</td></s<>	ub>3.5<
157	Deformation induced precipitation of MgZn2-type laves phase in Ti-Fe-Co alloy. Journal of Alloys and Compounds, 2019, 778, 795-802.	2.8	6
158	Circumventing the strength–ductility trade-off of β-type titanium alloys by defect engineering during laser powder bed fusion. Additive Manufacturing, 2022, 51, 102640.	1.7	6
159	Microstructure and mechanical properties of nanocrystalline WC-particle-reinforced Ti-based composites with nano/ultrafine-grained intermetallic matrix from spark plasma sintering and crystallization of amorphous phase. International Journal of Materials Research, 2012, 103, 613-619.	0.1	5
160	Influence of discharge plasma modification on physical properties and resultant densification mechanism of spherical titanium powder. Powder Technology, 2021, 389, 138-144.	2.1	5
161	Microstructure and oxidation resistance of CoNiCrAlY coating manufactured by laser powder bed fusion. Surface and Coatings Technology, 2021, 427, 127846.	2.2	5
162	Nano-amorphous—crystalline dual-phase design of Al80Li5Mg5Zn5Cu5 multicomponent alloy. Science China Materials, 0, , 1.	3.5	5

#	Article	IF	CITATIONS
163	Gravity-driven Beryllium Transport in ZrTiCuNiBe Melt and its Influence on Glass Formation. Journal of Materials Research, 2005, 20, 2302-2306.	1.2	4
164	Pressure effect on crystallization of Zr41Ti14Cu12.5Ni10Be22.5bulk metallic glass prepared by shock-wave quenching. Journal of Physics Condensed Matter, 2008, 20, 015201.	0.7	4
165	Serrated Flow Behavior of Titaniumâ€Based Composites with Different In Situ TiC Contents. Advanced Engineering Materials, 2015, 17, 1383-1390.	1.6	4
166	Novel AlEgens with a 3,5-dibromobenzaldehyde skeleton: molecular design, synthesis, tunable emission and detection application. Analytical Methods, 2018, 10, 5486-5492.	1.3	4
167	Microstructural Evolution and Mechanical Behavior of Lead-Free Silicon Brass Manufactured by Low-Pressure Die Casting. Journal of Materials Engineering and Performance, 2018, 27, 5478-5488.	1.2	4
168	Tailoring Grain Boundary and Resultant Plasticity of Pure Iron by Pulsed-Electric-Current Treatment. Metallurgical and Materials Transactions A: Physical Metallurgy and Materials Science, 2019, 50, 856-862.	1.1	4
169	Mechanical Properties of WC-Si3N4 Composites With Ultrafine Porous Boron Nitride Nanofiber Additive. Frontiers in Materials, 2021, 8, .	1.2	4
170	Silver Mesoporous Silica Nanoparticles: Fabrication to Combination Therapies for Cancer and Infection. Chemical Record, 2022, , e202100287.	2.9	4
171	In situ X-ray diffraction study on crystallization of shock-wave-quenched Zr-based bulk metallic glasses. Materials Science & Engineering A: Structural Materials: Properties, Microstructure and Processing, 2007, 449-451, 617-620.	2.6	3
172	Effects of Minor B4C or C on Amorphous Ti66Nb13Cu8Ni6.8Al6.2 Alloy Powders Synthesized by Mechanical Alloying. Journal of Inorganic and Organometallic Polymers and Materials, 2011, 21, 802-808.	1.9	3
173	Ultrahigh strength and large plasticity of nanostructured Ti 62 Nb 12.2 Fe 13.6 Co 6.4 Al 5.8 alloy obtained by selectively controlled micrometer-sized phases. Materials Characterization, 2017, 124, 260-265.	1.9	3
174	A Control Method of High Impact Energy and Cosimulation in Powder High-Velocity Compaction. Advances in Materials Science and Engineering, 2018, 2018, 1-11.	1.0	3
175	Correlation between microstructure and deformation mechanism in Ti66Nb13Cu8Ni6.8Al6.2 composites at ambient and elevated temperatures. Materials Science & Engineering A: Structural Materials: Properties, Microstructure and Processing, 2019, 767, 138448.	2.6	3
176	Research on microstructural and property evolution in laser cladded HAZ. Surface Engineering, 2021, 37, 1514-1522.	1.1	3
177	A novel yielding anisotropy and corresponding lattice evolution mechanism in CP-Ti achieved via pulsed electric current. Materials and Design, 2021, 209, 110013.	3.3	3
178	Comprehensive characterisation of tribo-layer in a Cu-15Ni-8Sn alloy during dry sliding wear. Materials Science and Technology, 2022, 38, 57-68.	0.8	3
179	WC-8Co-2Al (wt%) Cemented Carbides Prepared by Mechanical Milling and Spark Plasma Sintering. Materials Science Forum, 0, 638-642, 1817-1823.	0.3	2
180	Study on the discharge breakdown for carbonyl iron powder sintered by pulse electric current. Procedia Engineering, 2012, 27, 1434-1440.	1.2	2

#	Article	IF	CITATIONS
181	Effect of Minor Alloying Substitution on Glass-Forming Ability and Crystallization Behavior of a Ni ₅₇ Zr ₂₂ X ₈ Nb ₈ A (X = Ti, Cu) Alloy Synthesized by Mechanical Alloying. Materials Transactions, 2013, 54, 1844-1850.	.l&l t)stib&g	gt;5
182	Sinter-hardening with concurrent improved plasticity in iron alloys induced by spark plasma sintering. Journal of Materials Research, 2014, 29, 981-988.	1.2	2
183	Controlled synthesis of truncated octahedral bismuth micron particles with giant positive magnetoresistance. CrystEngComm, 2015, 17, 7056-7062.	1.3	2
184	Drop Tower Experiment to Study the Effect of Microgravity on Friction Behavior: Experimental Set-up and Preliminary Results. Microgravity Science and Technology, 2020, 32, 1095-1104.	0.7	2
185	Chemoimmunotherapy: Coordination and Redox Dualâ€Responsive Mesoporous Organosilica Nanoparticles Amplify Immunogenic Cell Death for Cancer Chemoimmunotherapy (Small 26/2021). Small, 2021, 17, 2170130.	5.2	2
186	Phase Transition of Shock-Loaded ZrTiCuNiBe Bulk Metallic Glass under Continuous Heating. Materials Transactions, 2008, 49, 869-873.	0.4	1
187	Fabrication of Ti ₆₆ V ₁₃ Cu ₈ Ni _{6.8} Al _{6.2} Bulk Composites with High Strength by Spark Plasma Sintering and Crystallization of Amorphous Phase. Advanced Materials Research, 2011, 284-286, 25-31.	0.3	1
188	Effect of zirconium on microstructures and mechanical properties of squeeze cast Al–5.0Cu–0.4Mn–0.1Ti–0.1RE alloy. Journal of Central South University, 2017, 24, 2231-2237.	1.2	1
189	Influence of Particle Size on Apparent Diffusivity During Spark Plasma Sintering of Crystalline Powders. Metallurgical and Materials Transactions B: Process Metallurgy and Materials Processing Science, 2019, 50, 2843-2852.	1.0	1
190	Effects of Applied Pressure on the Atomic Diffusion Coefficient During Spark Plasma Sintering of Crystalline Powders. Jom, 2019, 71, 2475-2483.	0.9	1
191	Tailoring chip morphology by correlating the microstructure and dynamic yield strength in turning of lead-free silicon brasses. Journal of Manufacturing Processes, 2020, 53, 420-430.	2.8	1
192	Reinjection flow field-flow fractionation method for nanoparticle quantitative analysis in unknown and complex samples. Journal of Chromatography A, 2021, 1638, 461897.	1.8	1
193	Editorial: Powder Sintering and Potential Applications. Frontiers in Materials, 2021, 8, .	1.2	1
194	Finite element simulation on mechanical properties of zeolite as a potential cellular structure. Journal of Physics: Conference Series, 2021, 2044, 012010.	0.3	1
195	Microstructure and mechanical properties of Ni50.7Ti49.3 shape memory alloy fabricated by selective laser melting. Journal of Physics: Conference Series, 2021, 2044, 012078.	0.3	1
196	Decomposition of cellular structure in selective laser melted Cu–Zn–Si silicon brass and its influence on microstructure, mechanical and corrosion properties. Materials Science & Engineering A: Structural Materials: Properties, Microstructure and Processing, 2022, 841, 143055.	2.6	1
197	Shear-accelerated crystallization of glass-forming metallic liquids in high-pressure die casting. Journal of Materials Science and Technology, 2022, 117, 146-157.	5.6	1
198	Uncovering electromigration effect on densification during electrical field assisted sintering. Journal of Materials Processing Technology, 2022, 307, 117630.	3.1	1

#	Article	IF	CITATIONS
199	Effect of proton irradiation on structure relaxation of Zr41.5Ti14.9Cu12.6Ni10.5Be20.4 bulk metallic glass. Science Bulletin, 2004, 49, 999-1001.	1.7	0
200	Synthesis of Nanocrystalline (W, Ti)C from Respective Elemental Powders by Mechanical Alloying and Spark Plasma Sintering. Advanced Materials Research, 0, 306-307, 1728-1734.	0.3	0
201	Electrochemical Treatment of Reverse Osmosis Concentrate of Oil Refining Wastewater by Mn-Sn-Ce/gamma-Al2O3 Particle Electrode. , 2012, , .		0
202	Microstructure and mechanical properties of TiNbFeCoAl alloys prepared by semi-solid sintering assisted by thermo-mechanical field. Vacuum, 2021, 190, 110316.	1.6	0
203	Effective Atomic Diffusion Coefficient Dependence on Applied Pressure During Spark Plasma Sintering. SSRN Electronic Journal, 0, , .	0.4	0
204	Effective Atomic Diffusion Coefficient Dependence on Applied Pressure During Spark Plasma Sintering. SSRN Electronic Journal, 0, , .	0.4	0
205	High-Performance TiBw/Ti Composite Prepared by Hot Extrusion. Journal of Physics: Conference Series, 2021, 2044, 012034.	0.3	0